NMR Solution Structure of a DNA 12/11-*mer*: d(CTCCTGTGTCTC)·d(GAGATA−AGGAG) Containing a Transplatin Interstrand G−N7/A−N1 Cross-Link

Bjørn Andersen,[a] Eloy Bernal-Méndez,[b] Marc Leng,[b] and Einar Sletten*[a]

Keywords: Oligonucleotides / Platinum / Molecular dynamics / NMR spectroscopy

The solution structure of a double-stranded DNA oligonucleotide, d(CTCCTG*TGTCTC)·d(GAGATA*–AGGAG), containing a *trans*-diammineplatinum(II) interstrand cross-link (the asterisks indicate the two cross-linked bases) has been determined by means of two-dimensional nuclear magnetic resonance (2D NMR) and NOE-restrained molecular dynamics and energy minimization refinement. The cross-linked duplex was prepared in two steps. First, *trans*-diamminedichloroplatinum(II) was reacted with the single-stranded d(CTCCTGTGTCTC), which resulted in the formation of a stable (G1,G3)-intrastrand cross-link. Then, the platinated oligonucleotide was hybridized with the partially complementary oligonucleotide d(GAGATA–AGGAG), in which the d(AT) doublet facing the intrastrand GTG cross-link replaced the d(CAC) triplet in a regular duplex. The formation of the hybrid promoted the rearrangement of the (G1,G3)-intrastrand cross-link into an interstrand cross-link. The NMR experiments were performed in 0.5 m NaCl solution. All the exchangeable and nonexchangeable proton resonances (except some H5′/H5′′ signals) of the major species could be assigned. NOESY spectra and chemical shift data indicate that the interstrand cross-link is established between G6–N7 and A18–N1. The platinated G residue is rotated about the glycosyl bond from an *anti* conformation into a *syn* conformation. The two imino protons G8–H1 and T17–H3 forming hydrogen bonds in the mismatched base pair, G8–T17, give rise to signals (upfield as expected) at δ = 10.52 and δ = 10.82. Using all the NOESY data (215 constraints) from a 0.8 mm sample, a solution structure of the cross-linked duplex has been obtained by NOE-restrained molecular dynamics/mechanics refinements. Only the central portion of the duplex deviates significantly from regular B-form geometry. The base residue T7 in the context GTG in the top strand is located in an extrahelical position. The interstrand cross-link induces a bend of 21° in the duplex.

Introduction

Recent years have witnessed the advent of oligonucleotides as tools for the modulation of gene expression. In the so-called antisense strategy, the binding of oligonucleotides to mRNA leads to inhibition of translation or RNA metabolism by two general mechanisms, namely the degradation of the targeted RNA by RNase H or the steric blocking of the cellular machinery.[1−8] Most studies in this area have dealt with RNase H-catalyzed cleavage of mRNA by phosphodiester oligonucleotides. However, a major drawback of these oligonucleotides is their rapid degradation by nucleases. They can be replaced by phosphorothioate oligonucleotides, which retain the ability to activate RNase H and are resistant to nucleases. Unfortunately, however, these are known to have side effects because of nonspecific binding to cellular proteins. An advantage of the steric blocking of cellular machinery is that chemically modified, and thus nuclease-resistant oligonucleotides can be used. However, a major constraint is that the oligonucleotide−RNA hybrids have to be sufficiently stable to avoid dissociation by the cellular machinery. Cross-linking of the oligonucleotides to their targets[1−8] can prevent such dissociation. Recently, a convenient method has been proposed for the specific and irreversible cross-linking of oligonucleotides to their targets in both cell-free and cell media. In this approach, *trans*-DDP [DDP: diamminedichloroplatinum(II)] modified oligonucleotides are used.[9]

In the reaction between *trans*-DDP and single-stranded oligonucleotides containing the triplet GNG (N being a nucleotide residue), (G1,G3)-intrastrand cross-links are formed. These intrastrand cross-links are stable as long as the oligonucleotides are single-stranded. There is, however, one exception.[10,11] It concerns intrastrand cross-links that have an adjacent C residue on the 5′ side. In the context d(CGNG) (N being A, T, or C), the following linkage isomerization occurs: *trans*-DDP [d(CGNG)−N7−G, N7−G] ⇄ *trans*-DDP [d(CGNG)−N3−C, N7−G]. Replacement of the C residue adjacent to the adduct on the 5′ side by a G, A, or T residue prevents this reaction.

Pairing of the single-stranded oligonucleotides containing a (G1,G3)-intrastrand cross-link with their complementary strands has two consequences. Firstly, the rearrangement of the (G1,G3)-intrastrand cross-link to the

[a] Department of Chemistry, University of Bergen, Allégt. 41, N-5007 Bergen, Norway
Fax: (internat.) + 47/55589490
E-mail: Einar.Sletten@kj.uib.no
[b] Centre de Biophysique Moléculaire, CNRS, Rue Charles Sadron, F-45071 Orleans Cedex 02, France
Fax: (internat.) + 33-2/38631517
Supporting information for this article is available on the WWW under http://www.wiley-vch.de/home/eurjic or from the author.

  1434−1948/00/0606−1201 $ 17.50+.50/0

(C1,G4)-intrastrand cross-link is blocked. Secondly, another linkage isomerization reaction is triggered by the formation of the double helix, which involves rearrangement of the (G1,G3)-intrastrand cross-link into an interstrand cross-link. This rearrangement occurs irrespective of the nature of the nucleotide residues adjacent to the intrastrand cross-link.[9,12−14]

The mechanism of the rearrangement is not yet known in detail, although some points have been established.[12−14] In the interstrand cross-link, only the 5′G (and not the 3′G) of the former intrastrand cross-link is involved. The interstrand cross-linking reaction does not proceed through a solvent-associated intermediate. Cleavage of the Pt−3′G bond with formation of a monofunctional adduct can be excluded. Direct nucleophilic attack of the Pt−3′G bond by either the C residue complementary to 5′G, or the A residue if the triplet complementary to the intrastrand cross-link is replaced by the doublet d(TA) or r(UA), has been suggested. At 37 °C, the rate of the interstrand cross-linking reaction depends on several parameters, such as the shape of the double helix and the sequence of the targeted oligonucleotide. The fastest reaction (complete within a few minutes) occurs in the hybrids between platinated oligo(2′-*O*-Me)nucleotides and RNA containing the doublet UA facing the platinated triplet.

Our envisaged uses of the *trans*-DDP-modified oligonucleotides are as tools in molecular biology and as drugs for modulating gene expression. In both cases, the requisite oligonucleotides have to be designed, which implies a complete knowledge of the interstrand cross-linking reaction. Knowledge of the structures of the cross-linked duplexes is thus essential, which prompted us to undertake a systematic study of the structures of these duplexes. In this paper, we report on a structure determination of a *trans*-DDP interstrand cross-linked DNA duplex. The system investigated in detail consists of a 12/11-*mer* hybrid d(CTCCTG*TGTCTC)·d(GAGATA*−AGGAG) (the asterisks indicate the cross-linked bases), in which the lower strand differs from the regular complementary strand in that the CAC triplet complementary to the platinated GTG triplet is replaced by the doublet d(TA). The interstrand cross-linked product has been characterized by NMR spectroscopy and a combination of NOESY-restrained molecular dynamics and energy minimization refinement.

Results

Synthesis of the Cross-Linked Duplexes

A scheme showing the synthesis of a duplex incorporating an interstrand cross-link is given in Figure 1, a. The progress of the cross-linking reaction was monitored by FPLC analysis (Figure 1, b), which showed that after 9 days it had almost reached completion. The ^{1}H-NMR spectrum of the sample obtained following FPLC purification featured one set of major resonances as well as some small signals due to a minor component (< 3%) (Figure 2, a). When the spectrum was recorded a few days later, the resonances attributable to the minor component had increased to ca. 14% (Figure 2, b). The signals due to this minor species were not characterized further by NMR analysis because of a low spectral signal-to-noise ratio. Subsequently, the salt concentration was increased to 0.5 M NaCl, which led to an appreciable reduction in the amount of the minor component, its concentration returning to a level comparable to that seen in the initial spectrum (< 3%). This suggests a salt-induced shift in the conformational equilibrium in favor of the major component. The melting temperature for the cross-linked duplex in 0.150 M NaCl was found to be 62 °C, and probably a few degrees higher in 0.500 M NaCl.

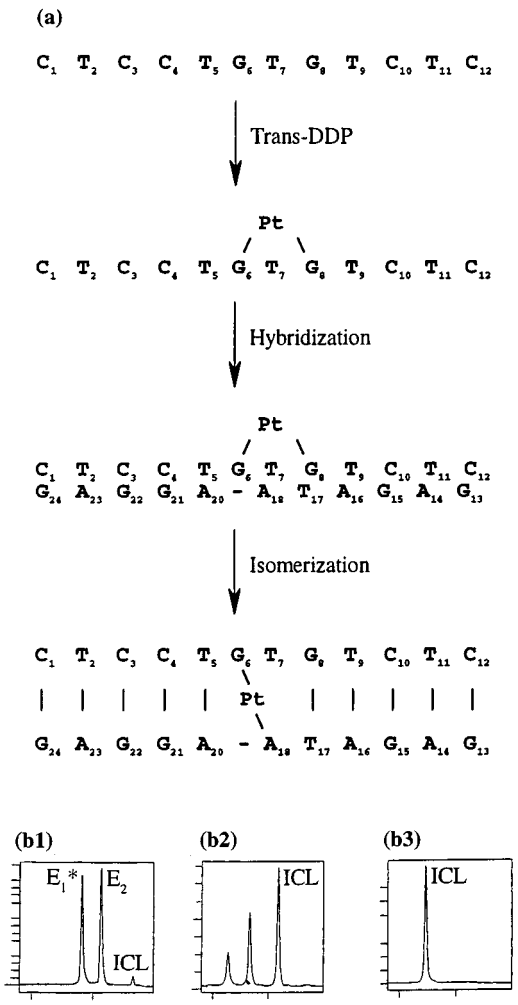

Figure 1. (a) Scheme of the cross-linking reactions; (b) FPLC elution profiles of the isomerization process from intrastrand to interstrand cross-linked (ICL) duplex: (b1) intrastrand cross-linked oligonucleotide (E_1*) mixed with its complementary sequence (E_2), (b2) a few days after mixing, (b3) FPLC-purified interstrand cross-linked (ICL) duplex

NMR Assignments

Comparison of the aromatic−H1′/H5 regions of the NOESY spectra of the platinated (Figure 3) and nonplatinated duplex (Figure 4) reveals dramatic changes in the chemical shift patterns. It is difficult to directly compare the

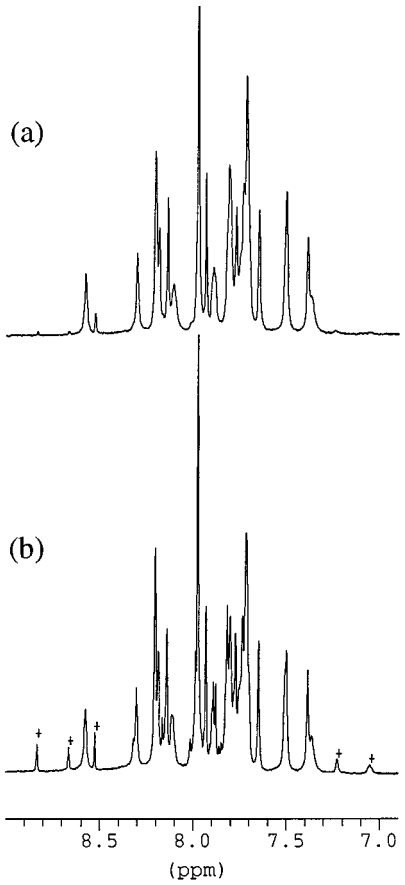

Figure 2. The downfield region of the 600 MHz ^{1}H-NMR spectrum of the *trans*-DDP cross-linked duplex d(CTCCTG*TGTCTC)·d(GAGATA*−AGGAG) (the asterisks * indicate the cross-linked bases) in D_2O at 305 K; (a) freshly prepared sample, (b) one week later; the signals attributable to the minor component are marked with +

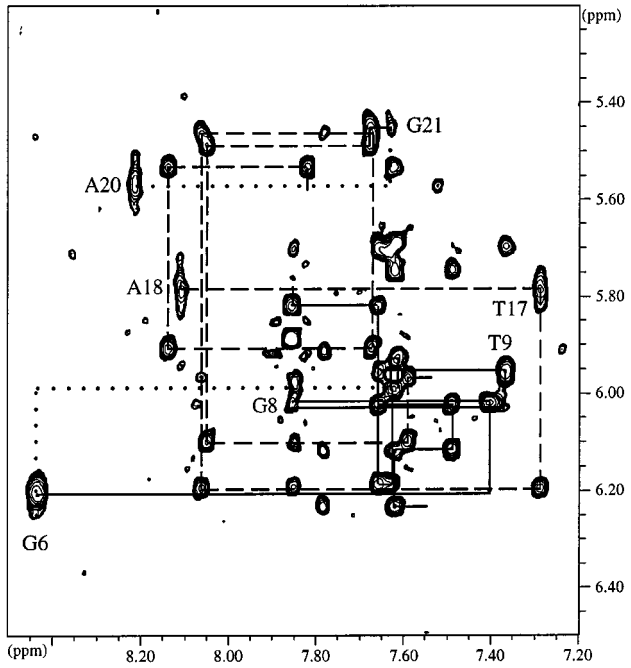

Figure 3. Contour plots of the resolution-enhanced H8/6−H1′/H5 region in the 600 MHz NOESY spectra of the *trans*-DDP cross-linked duplex d(CTCCTG*TGTCTC)·d(GAGATA*−AGGAG); the sequential connectivities are indicated with solid lines for the upper strand and broken lines for the lower strand, while absent connectivities are shown with dotted lines; the mixing time was 200 ms and the temperature 290 K

number of observed cross-peaks due to the large concentration difference, i.e. 0.8 mM and 3 mM, respectively. The non-exchangeable proton resonances were assigned following standard procedures; most of the sequential connectivities could be observed in the cross-peaks in the different spectral regions, i.e. aromatic−H1′/H3′, and aromatic−aromatic. Cross-peaks arising from traces of nonplatinated oligomers could be identified by comparison of NOESY maps of the duplex before and after platination. As expected, the 2D NOESY map of the platinated species shows a substantial downfield shift of the signal due to H8 of the cross-linked G6 residue. The chemical shift of adenine A18−H8, the cross-linked residue on the lower strand, is found in the normal range for H8 protons of nonplatinated A−N7. In the expanded portion of the downfield region of the 1D proton spectrum, two broad partially overlapping signals are observed at $\delta = 8.43$ and $\delta = 8.45$. By reference to the NOESY spectra, these resonances were assigned to the downfield shifted G6−H8 and A18−H2 protons of the platinated G and A residues, respectively. The DQF-COSY data were not of sufficient quality to yield reliable coupling constants for the sugar region due to severe overlap. The exchangeable proton resonances were assigned on the basis of the 1D spectra (Figure 5) and 2D NOESY spectra of the imino−imino and amino−aromatic regions. The chemical shifts of the assigned resonances of the platinated and non-platinated duplexes are listed in Table 1.

The NMR data for the 13/12-*mer* cross-linked duplex, which has an extra GC base pair, are almost identical to those obtained for the 12/11-*mer* (data not shown). The idea of extending the sequence was to increase the thermal stability of the duplex and thus to improve the quality of the spectral data. However, a comparison of the imino regions of the 12/11-*mer* and the 13/12-*mer* reveals only marginal improvement (data not shown).

The most prominent features in the spectra are the large downfield shifts of G6−H8 ($\delta = 8.43$) and A18−H2 ($\delta = 8.45$), which confirm that the cross-link is established between G6−N7 and A18−N1. The large intranucleotide G6−H8···H1′ crosspeak (Figure 3) corresponds to a *syn* conformation, which is probably adopted as a result of the platination. The H8/H1′ cross-peaks involving the adenine residues A18 and A20 are elongated, reflecting the rather flexible conformation at 290 K.

The connectivities involving adenine H2 protons are important in determining the global structure. The signal-to-noise level in the NOESY spectra of the nonplatinated duplex allows us to identify several H2···H1′ contacts of the type H2(n)···H1′(n), H1′(n+1), H1′(m+1), H1′(m), where n and m refer to complementary residues in a base pair. The H2(n)···H1′(m) distance in a regular Watson−Crick base pair is approximately 5.1 Å and the cross-peak correspond-

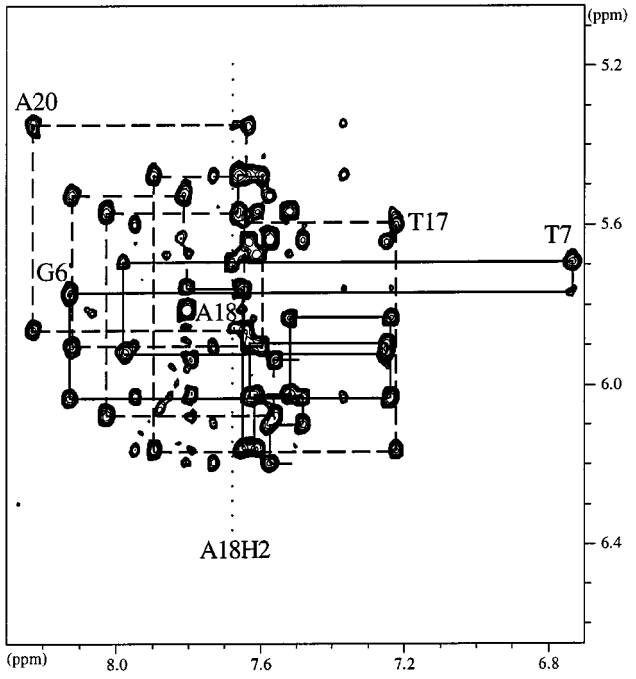

Figure 4. Contour plots of the resolution-enhanced H8/6−H1′/H5 region in the 600 MHz NOESY spectra of the nonplatinated duplex; the sequential connectivities are indicated with solid lines for the upper strand and broken lines for the lower strand, while absent connectivities are shown with dotted lines; the mixing time was 200 ms and the temperature 290 K

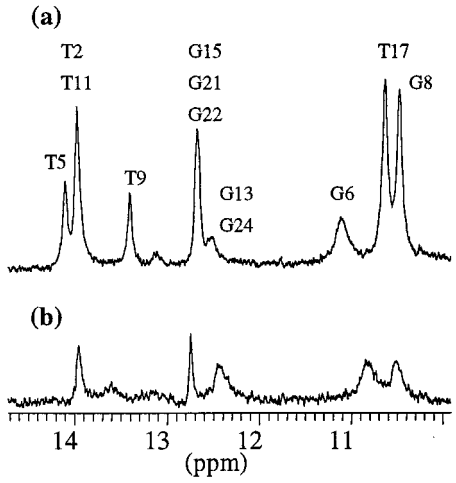

Figure 5. Imino proton resonances of the duplex d(CTCCTG*TGTCTC)·d(GAGATA*−AGGAG) at 290 K; (a) nonplatinated and (b) *trans*-DDP platinated

ing to such a long distance is not normally observed in NOESY maps. In the platinated form, H2(n)···H1′(m+1) cross-strand contacts are observed between A14/C12, A16/C10, and A23/C3.

The proton resonances of two of the thymine residues, T7 and T17, are of particular importance since these are involved in atypical duplex geometry. Thymine T7 may be located either in a bulged extrahelical position or stacked in the helix. Thymine T17 is partner in a GT mismatched base pair and thus might exhibit unusual chemical shifts. The methyl resonance of T7 is very weak, indicating a high degree of conformational motion. No cross-peaks in the aromatic−aromatic region involving T7−H6 are detected, suggesting that T7 is looped out of the double helix. The chemical shifts of the thymine T17 protons are, however, compatible with a regular B-DNA geometry.

The ^{1}H-NMR spectrum of the exchangeable protons in H_2O solution is rather noisy at 290 K (Figure 5). At lower temperatures, the situation is not improved due to extensive signal broadening at the relatively high salt concentration (0.5 M NaCl). The imino resonances of G8 and T17 are, however, easily recognized by virtue of their expected upfield positions at $\delta = 10.52$ and $\delta = 10.82$, characteristic for a mismatched base pair. Due to the low signal-to-noise level in the NOESY map, not all of the imino resonances could be assigned unambiguously.

^{31}P-NMR spectra of the nonplatinated and platinated duplexes are shown in Figure 6. It was not possible to assign the resonances on the basis of the available data. For the nonplatinated duplex, we had expected a downfield shifted resonance for the extrahelical thymine residue. However, the resonance patterns for both the nonplatinated and platinated duplexes, centered at about $\delta = -4.1$ and with no downfield shifted resonances, are indicative of a range of phosphate conformations consistent with regular DNA geometry.

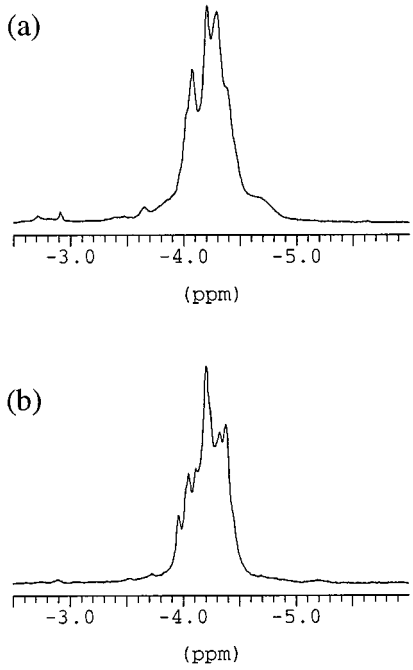

Figure 6. ^{31}P-NMR spectra of the duplex d(CTCCTG*TGTCTC)·d(GAGATA*−AGGAG) at 290 K; (a) nonplatinated and (b) *trans*-DDP platinated; shifts referenced to trimethyl phosphate

Molecular Modelling

Many cycles of subsequent interactive geometry refinements starting from regular B-DNA geometry converged at a model, the simulated NOESY spectra for which were in satisfactory agreement with the experimental spectra, as

Table 1. ^{1}H-NMR chemical shifts (ppm) for the *trans*-DDP cross-linked duplex d(CTCCTG*TGTCTC)·d(GAGATA*−AGGAG); the differences in the chemical shifts between the platinated and nonplatinated duplex are given below the chemical shifts; all shifts are referenced to the HOD resonance at δ = 4.84, T = 290 K

	H6/H8	H2/H5/CH_3	H1′	H2′	H2′′	H3′	H4′	H1/H3	Hf	Hb
C1	7.86	5.89	5.82	2.24	2.54	4.63	4.08		7.06	7.75
	0.06	0.08	0.07	0.00	0.00	0.03	0.03		0.20	0.10
T2	7.66	1.66	6.19	2.26	2.60	4.91	4.29	13.95		
	0.02	0.03	0.03	0.03	0.01	0.02	0.05	0.04		
C3	7.62	5.71	5.99	2.16	2.48	4.88	4.24		6.88	8.37
	0.03	0.04	−0.04	0.00	−0.03	0.02	0.00		0.06	0.12
C4	7.60	5.69	5.92	2.14	2.48	4.82	4.22		7.01	8.30
	0.08	0.12	0.09	0.18	0.03	0.09	0.09		0.17	0.07
T5	7.60	1.84	6.01	2.25	2.48	4.84	4.27	–		
	0.36	0.26	−0.02	0.48	0.19	−0.13	0.25	–		
G6	8.44		6.20	2.26	2.62	4.96	4.36	–	–	–
	0.31		0.43	−0.22	−0.08	0.51	0.22	–	–	–
T7	7.40	1.55	6.02	2.32	2.37	4.85	4.12	–		
	0.67	0.57	0.33	0.52	0.08	0.19	0.14	–		
G8	7.85		6.02	2.50	2.69	4.90	4.19	10.52	–	–
	−0.13		0.10	−0.24	−0.14	0.00	−0.14	0.14	–	–
T9	7.36	1.60	5.96	2.18	2.48	4.83	4.19	13.60		
	0.10	0.17	0.06	0.04	−0.02	0.06	−0.02	0.43		
C10	7.66	5.70	6.02	2.14	2.48	4.78	4.09		7.05	8.34
	0.04	0.06	−0.01	−0.01	−0.03	0.00	−0.10		0.14	0.06
T11	7.49	1.72	6.12	2.17	2.48	4.86	4.08	13.95		
	0.01	0.03	0.02	0.01	−0.02	0.00	−0.08	0.04		
C12	7.62	5.75	6.23	2.27	2.28	4.55	4.01		7.14	8.08
	0.05	0.10	0.03	0.00	0.00	0.00	0.02		0.36	−0.13
G13	7.82		5.53	2.42	2.61	4.80	4.14	12.45	–	–
	0.01		0.01	−0.04	−0.06	0.00	−0.02	0.00	–	–
A14	8.14	7.79	5.91	2.67	2.77	5.01	4.37		–	–
	0.02	0.06	0.01	0.00	−0.05	0.00	0.01		–	–
G15	7.67		5.46	2.50	2.65	4.94	4.32	12.75	–	–
	0.09		−0.02	0.08	0.09	0.01	0.01	0.17	–	–
A16	8.06	7.65	6.20	2.50	2.65	4.91	4.39		–	–
	0.16	−0.30	0.04	0.14	−0.09	−0.01	−0.01		–	–
T17	7.29	1.66	5.79	1.97	2.08	4.74	3.96	10.82		
	0.07	0.31	0.19	−0.18	−0.17	−0.09	−0.17	0.23		
A18	8.11	8.45	5.80	2.30	2.38	4.72	3.95		–	–
	0.47	0.80	−0.06	−0.14	−0.12	−0.13	−0.26		–	–
A20	8.22	7.52	5.57	2.69	2.71	5.00	4.30		–	–
	−0.01	0.15	0.21	0.09	0.06	0.07	0.03		–	–
G21	7.63		5.45	2.50	2.58	4.94	4.30	12.75	–	–
	0.02		−0.03	−0.01	−0.03	0.07	−0.01	0.17	–	–
G22	7.68		5.49	2.50	2.65	4.93	4.28	12.7	–	–
	0.02		−0.08	−0.01	−0.05	−0.03	−0.05	0.12	–	–
A23	8.05	7.85	6.10	2.60	2.86	5.00	4.40		–	–
	0.02	0.07	0.02	0.02	−0.01	0.00	0.00		–	–
G24	7.59		5.95	2.25	2.36	4.61	4.16	12.4	–	–
	0.03		0.01	0.00	0.00	0.01	0.02	0.00	–	–

judged by visual inspection. Figure 7 shows a comparison between the simulated and experimental spectra for the aromatic-H1′/H5/H3′ and aromatic-aromatic regions. All the NOESY peaks in the simulated spectra are observed in the experimental spectra, except for the cross-peaks corresponding to A18-H2G8-H8 and A20-H2G6−H8. This may be explained by partial saturation of the NOE signals involving A−H2 due to the short (2 s) relaxation delay. The overall agreement is, however, quite satisfactory. Some minor residual cross-peaks are apparent, corresponding to the H-bonded amino protons that have not been completely exchanged with deuterium, as well as a few cross-peaks that are presumably attributable to the minor component. A refinement starting from A-DNA geometry also led to an excellent fit between the simulated and experimental NOESY spectra, although the global bending for this model was larger than that in the case of a refinement starting from B-DNA.

Stereoviews of the refined structure (Figure 8) and a close-up of the central section of the duplex (Figure 9) are presented. The main feature to be noticed is the G6−N7···A18−N1 cross-link, which is accommodated within the duplex with retention of the overall B-DNA geometry. The ammonia ligands are seen to form hydrogen bonds to T5−O2 (2.70 Å) and T17−O4 (3.27 Å), respectively. In addition, both ammonia ligands are located in hydrophilic pockets and show several close contacts in the range 2.4−3.3 Å. The extra residue, thymine T7, is seen to loop out of the helix, giving it added conformational flexibility. The adenine A18 platination site could, in principle, involve either N7 or N1. Both models were tested in the refinement, but only the latter gave a reasonable fit to the NOE data. Additional support in favor of A−N1 involvement is provided by a related system where the cross-linking reaction rate is retarded when UA is replaced by the UG doublet.[13]

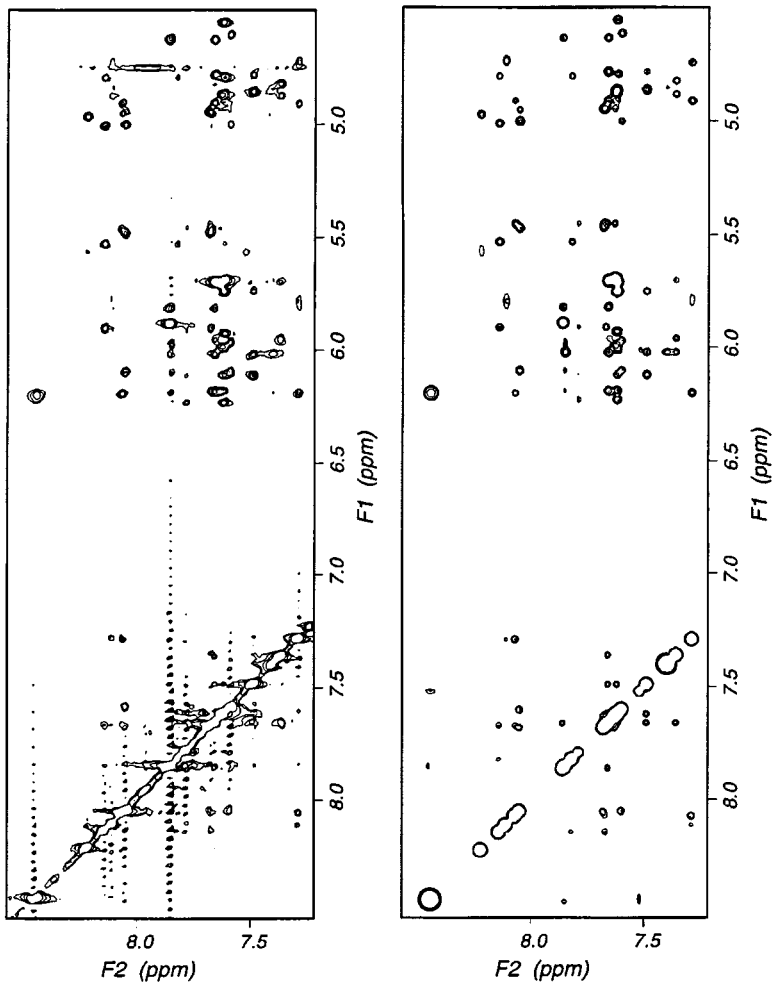

Figure 7. Expanded regions of the nonexchangeable proton 2D NOESY spectra of the *trans*-DDP cross-linked duplex d(CTCCTG*TGTCTC)·d(GAGATA*−AGGAG; left: experimental spectra: aromatic−aromatic region and aromatic−H1′/H3′ region; right: the corresponding simulated spectra

The helix is bent by 21°, as measured by the angle between the two helix axes calculated by CURVES[15] through residues 1−5 and 8−12, respectively, excluding residues G6, T7, and A18. The stacking interactions between the bases are maintained throughout the duplex except for those involving residues G6 and T7. The simulated NOESY data fit quite well with the experimental data representing the stacking region (aromatic−aromatic, Figure 7). The interplanar distances for the stacked bases were calculated by CURVES to lie in the range 2.7−3.8 Å. A complete listing of helical parameters is available as supplementary material.

Watson−Crick hydrogen-bonding is maintained for 10 of the 11 possible combinations. As expected, the platinated residues G6 and A18 are not involved in hydrogen bonding. The mismatched GT base pair, on the other hand, forms two quite regular N−H···O bonds. The chemical shifts of the two imino protons involved were observed at the expected upfield positions. The regular hydrogen-bonded base pairs have a negative propeller twist in the range −19° to −45°. Similar values have been observed in other duplex DNA oligonucleotides.[16] The mismatched base pair, G8−T17, has a positive propeller twist of 35°. The helical parameters are generally not well-defined, mainly due to a low signal-to-noise level in the 2D NOESY spectra obtained from the rather dilute (0.8 mM sample), and are not sufficiently precise for a high-quality structure determination.

Discussion

The 1,3-intrastrand cross-links between *trans*-DDP and two guanine residues separated by one base are relatively stable under single-strand conditions[10,11] and rearrange into interstrand cross-links when the platinated oligonucleotides are annealed with their complementary strands.[12−14] The different rates observed for such cross-linking reactions can be rationalized in terms of the relative positions of the attacking nucleotide residue and the platinum residue as well as the chemical nature of the attacking nucleotide residue. It is important to determine the local conformation of the double helix in these platinated species for several reasons, e.g. to establish the link between geometric factors and the rate of the interstrand cross-linking reaction.

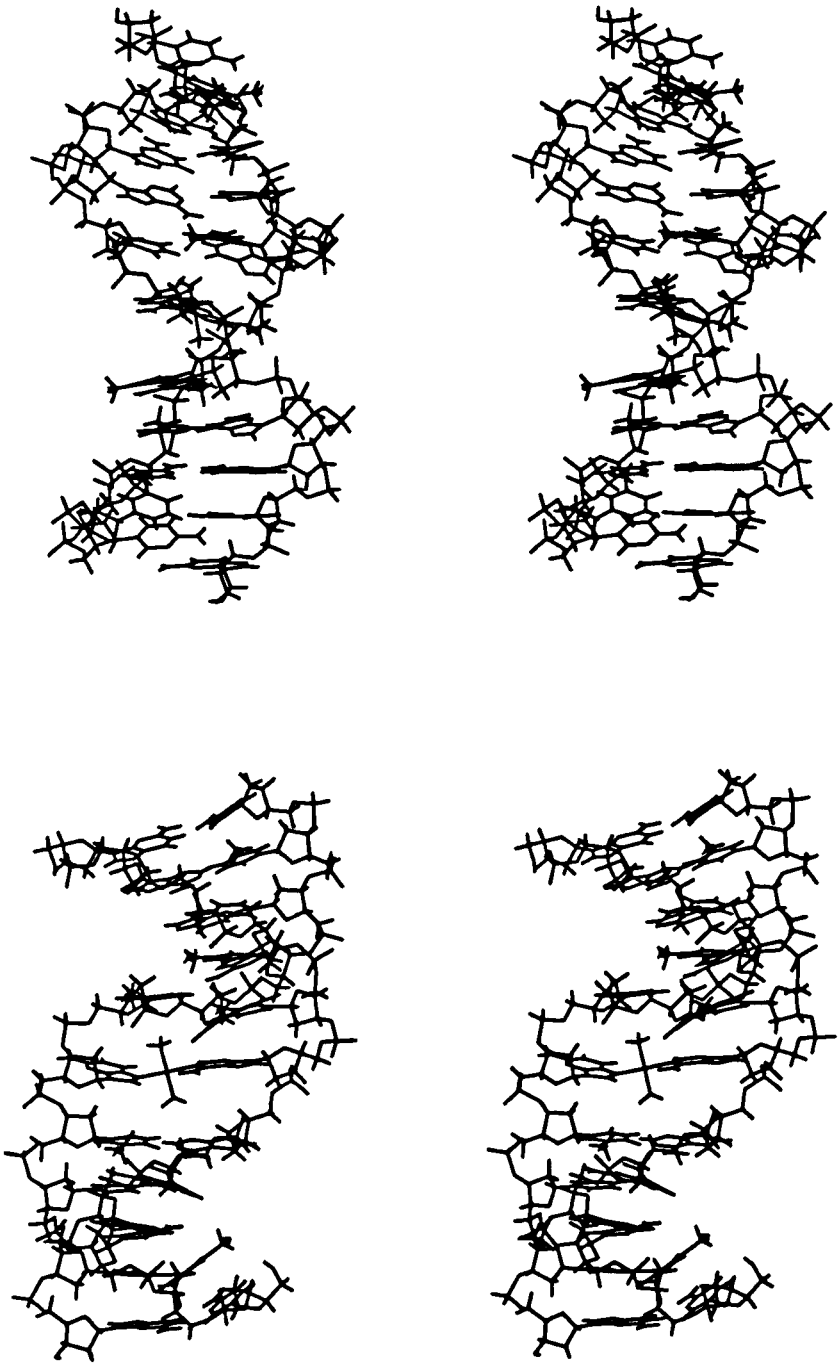

Figure 8. Stereoviews of the molecular model of the refined *trans*-DDP interstrand cross-linked duplex d(CTCCTG*TGTCTC)·d(GAGATA*−AGGAG)

The occurrence of both a major and a minor component of the cross-linked duplex, their contributions depending on time and the electrolyte concentration, indicates that a reversible conformational equilibrium is established. The minor component has not been further characterized by NMR analysis, thus the nature of these salt-induced structural changes has not been delineated. HPLC analysis and capillary electrophoretic measurements of the sample several weeks after the NMR data had been recorded revealed that the major cross-linked species was in fact accompanied by three minor constituents (3−9%).

Two broad downfield-shifted resonances at $\delta = 8.45$ and $\delta = 8.43$ were assigned to A18−H2 and G6−H8, respectively. Most of the NMR-based structural information currently available on platinum−DNA adducts pertains to *cis*-DDP, whereas only a few structural investigations of *trans*-DDP−DNA have been performed. Platination of purine N7 is predicted to induce a downfield shift of the H8 signal by ca. 0.5 ppm as a result of an inductive effect,[17] with a further contribution from conformation-dependent effects of the environment. In a study of *trans*-DDP adducts of d(GpTpG) platinated at N7, the downfield shifted G−H8

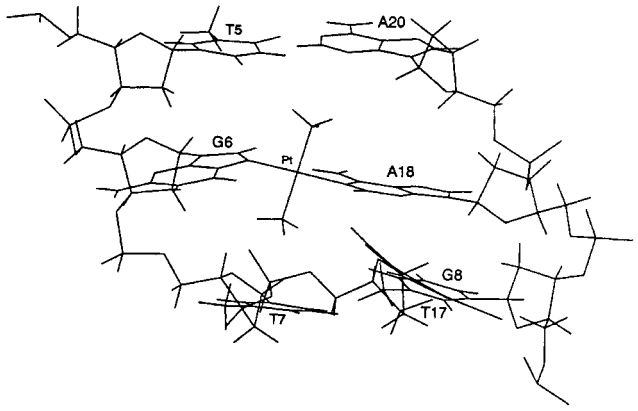

Figure 9. View of the central part of the platinated duplex

signal was observed at $\delta \approx 8.7$ (300 K).[18] In the single-stranded d(A*GG*CCT) containing the 1,3-*trans*-DDP adduct at A1−N7 and G3−N7, the signals of the aromatic protons A−H8 and G−H8 are observed at $\delta = 9.3$ and $\delta = 8.7$, respectively.[19] There is no corresponding example of an oligonucleotide *trans*-DDP-modified at A−N1, although in a study of the isomers d(GpA) and d(ApG), *cis*-DDP-modified at G−N7 and A−N1, downfield shifted A−H2 signals were observed at $\delta = 8.75$ and $\delta = 9.00$, respectively.[20]

From the NOESY spectra, it is evident that the residues adjacent to the platinated sites have a high degree of flexibility. The H8···H1′ cross-peaks involving residues A18 and A20 are especially poorly defined and provide only qualitative interatomic distance information. A sequential "walk" including *intra*- and *inter*-nucleotide connectivities in the aromatic−H1′ region can be completed for most of the residues, except for G6−H8···T7−H1′ in the upper strand and A18−H8···A20−H1′ in the lower strand. The NOESY maps for the 13/12-*mer* cross-linked duplex, which has an extra GC base pair, show essentially the same shift and connectivity pattern as for the 12/11-*mer*, thus excluding the possibility of any artifacts due to the duplex being too short.

The molecular structure of the platinated duplex shown in Figure 8 is based on NMR spectroscopy and restrained molecular dynamics and energy minimization calculations. In general, it has been observed that extrahelical pyrimidine bases tend to destack, while extrahelical purine bases stack with the nonplatinated duplexes.[21,22] However, in the NOESY spectrum of the nonplatinated duplex (Figure 4) the H6 resonance of thymine T7 in the context −GTG− is observed in an extreme upfield position, which suggests a high degree of deshielding in a base-stacked environment. In the platinated duplex, this thymine residue is looped out of the helix, although its exact location is not well-defined since T7 is involved in only a few NOE constraints. The fact that pyrimidine T7 is looped out leaves more room for the G6 residue to adopt a nonregular conformation, which may facilitate the interstrand cross-linking reaction. Kinetics experiments have shown that the rate of the interstrand cross-linking reaction is independent of the nature of the intervening base between the two cross-linked G residues in the top strand.[12−14]

The interstrand cross-link causes a local distortion of the double helix and induces a bend (21°) of its axis towards the major groove. However, it is generally accepted that the determination of global bending by NMR methods is rather inaccurate.[23] It is remarkable that the base pairs flanking the interstrand cross-links adopt a regular B-DNA conformation and that the distortion is located at the level of the cross-link. A similar conclusion has been reached in the case of duplexes containing a *cis*-DDP interstrand cross-link,[24−26] although the local distortions induced by *cis*- and *trans*-DDP are quite different.

Finally, an interesting aspect of this study is the fact that one of the amino groups of the Pt residue protrudes into the minor groove of the cross-linked duplexes (Figure 8). Both of the NH_3 ligands are seen to form hydrogen bonds to adjacent base residues (T5, T17), although one of the NH_3 ligands is less constrained and more exposed to the solvent. This suggests that the cross-linked duplexes should be able to accommodate larger nonleaving groups (L), which, in turn, may facilitate the cross-linking reaction and stabilize the platinated duplexes. Work is currently in progress with *trans* complexes of the general formula *trans*-$[Pt(NH_3)LCl_2]$.

Concluding Remarks

This work deals with structural characterization of a Pt−DNA duplex posing several nonroutine obstacles: (i) the duplex is made up of nonpalindromic sequences (giving a double set of resonances), (ii) a residue is missing from the complementary strand, (iii) the sample is dilute (0.8 mM) and furthermore contains several minor species, leading to a decreased signal-to-noise level. Thus, the task represents a real challenge to the standard NMR procedures for structure determination of oligonucleotide duplexes. In comparison with other NMR determinations of regular, platinated and nonplatinated oligonucleotides, the accuracy of the present structure is consequently expected to be lower. However, the main objective of this investigation has been achieved, i.e. to qualitatively determine the cross-linking arrangement in order to be able to suggest modifications to further speed up the cross-linking reaction rate.

Experimental Section

Sample Preparation: All the sequences were purchased from Oswell DNA Service as HPLC purified compounds. The reactions between *trans*-DDP and the pyrimidine-rich strands d(CTCCTGTGTCTC) (I) and d(CTCCTGTGCTCTC) (II) containing the GTG sites were performed as described previously.[12,14] Briefly, the single-stranded oligonucleotides ($c = 40$ μM) were incubated with 1.1 equivalents of *trans*-DDP in 10 mM $NaClO_4$/4 mM acetate buffer at pH 3.6 and

37 °C over a period of 24 h. Thereafter, the reaction mixtures were treated with thiourea (10 mM) for 10 min at 37 °C. The oligonucleotides containing a single 1,3-*trans*-{$Pt(NH_3)_2$[d(G*TG*)]} cross-link were purified by chromatography on a strongly basic anion-exchange resin on a Pharmacia FPLC system equipped with a MonoQ column, using a 0.2 to 0.7 M NaCl gradient in 10 mM NaOH. The binding of the platinum at the G residues was verified by the nonreactivity of dimethyl sulfate towards these sites.[12,14]

The platinated oligonucleotides were mixed with one equivalent of the complementary sequence, d(GAGATA−AGGAG) or d(GAGAGTA−AGGAG), respectively. Then, the duplexes (20 μM final concentration) in 500 mM NaCl, 10 mM Tris-HCl buffer (pH 7.5), and 0.5 mM EDTA were incubated at 288 K. After 9 days, the intrastrand to interstrand cross-link isomerization reactions were complete. The interstrand cross-linked duplexes were subsequently purified by chromatography on a strongly basic anion-exchange resin and then desalted on a Sep-Pak Column. The platinated 12/11-*mer* NMR sample was made up from 0.5 mL of the 0.8 mM in duplex solution in 0.5 M NaCl and 0.04 mM EDTA, and the pH was adjusted to 5.9. No buffer was added. The sample of the non-platinated duplex was dissolved in 0.55 mL of 9:1 H_2O/D_2O containing 0.520 M NaCl (pH 5.9) so that the final duplex concentration was 3.0 mM. ^{1}H-NMR spectra were recorded in H_2O solution and subsequently in D_2O after freeze-drying of the samples and redissolving them in 99.996% D_2O.

NMR Spectroscopy: The ^{1}H NMR experiments were performed on a Bruker DRX 600 instrument operating at 600 MHz for ^{1}H. In order to avoid melting of the duplexes and to obtain reasonable resolutions, all experiments were carried out at 290 K. 1D ^{1}H spectra were acquired with a total of 32 K complex points and 64 scans. For all 1D and 2D spectra, the spectral widths were 6000 Hz (in D_2O) or 13200 Hz (in H_2O) and a relaxation delay of 2 s was used. The 3-9-19 WATERGATE pulse sequence was used for water suppression.[27] The ^{1}H NOESY spectra were recorded in the pure absorption mode with quadrature detection using the States TPPI acquisition scheme.[28] A total of 2048 complex points in t_2 were collected for each of 512 t_1 increments and 80 transients were averaged for each increment. 2D NOESY spectra were acquired at four different mixing times (75, 125, 200, and 300 ms) in D_2O and in H_2O. The FIDs were processed by linear prediction routines increasing the time domain to 4 K, which significantly improves the signal-to-noise in the NOESY map.[29] DQF-COSY experiments were performed by collecting 2048 data points in t_2 and 512 data points in t_1, and the data were zero-filled to 2 K in both directions. The NMR data were processed on a Silicon Graphics INDY workstation using the program FELIX (Biosym)[30] and on a 133 MHz Pentium PC using 1D and 2D WIN-NMR (Bruker).[31] The one-dimensional ^{1}H FIDs were multiplied by an exponential window function prior to Fourier transformation. Typically, 1 Hz was added to the line widths. No baseline correction was needed. The two-dimensional NOESYs, which were used for integration, were apodized by a sinebell filter function, while assignments were made from resolution-enhanced spectra using a Gaussian function. The proton spectra were referenced to the HOD resonance at δ = 4.84 (290 K). ^{31}P-NMR spectra of the platinated and nonplatinated duplexes were acquired at 242.94 MHz. T_1 spin-lattice relaxation times were determined by the inversion recovery method.

NOE Distance-Restrained Molecular Dynamics/Mechanics Refinement: Nonexchangeable proton−proton distances were derived from initial NOE build-up rates as a function of mixing times using the cytosine H5−H6 distance of 2.46 Å as a reference. Cross-peaks were selected and integrated using WIN-NMR (Bruker). The thymine methyl (pseudo atom)−H6 distances were fixed at 3.1 Å. For all the N···H bonds, lower and upper limits of 1.7 Å and 2.0 Å, respectively, were used, while corresponding limits of 1.8 Å and 2.2 Å were used for O···H bonds. The platinum was attached to G6−N7 and A18−N1 at a fixed Pt−N distance of 2.0 Å. The square-planar coordination geometry about the metal was completed by two NH_3 ligands in *trans* positions. Charges on the metal and its NH_3 ligands were set in accordance with previous work by Kozelka et al.[32] Restrained molecular dynamics were conducted using the AMBER all-atom force field as implemented in DISCOVER (3.1) software. The calculations were carried out in vacuo with a distance-dependent dielectric constant of the form 4*r* and a force field with all 1−4 nonbonding interactions scaled by a factor of 0.5.[33]

The force constants used for the hydrogen bonds were set to 25 mol^{-1} $Å^{-2}$. For the other constraints, a force constant of 20 kcal mol^{-1} $Å^{-2}$ was applied when the relevant distances were outside of their limits. This approach is in accordance with recent work by Jourdan et al.[34] All dynamics calculations were performed on a Silicon Graphics INDY workstation using the programs INSIGHT II, DISCOVER, and NMR Refine (Biosym).[33] The calculation began with both classical A-DNA and B-DNA as modelled in INSIGHT II. The platinated guanine residue G6 was rotated into a *syn* configuration, in agreement with the derived intranucleotide G6−H8···H1′ NOE distance.

A total of 215 NOE distance constraints were used in the energy refinements of the starting models (A- and B-form DNA) using a conjugate gradient minimization algorithm. Initially, 500 cycles of energy minimization followed by 20 ps of molecular dynamics calculations at a constant temperature of 300 K were performed. The Verlet Leapfrog[35] algorithm was used to integrate the equations of motion, with an integration step of 1 fs. The average calculation frequency was 10 steps. The DISCOVER program uses Berendsens method[36] for pressure control. The molecular dynamics calculation was followed by a second run of 2000 cycles of energy refinement until an average rms gradient of 0.06 kcal mol^{-1} $Å^{-2}$ had been achieved. NMR Refine (Bruker) was used to generate the NOESY cross-peak volumes, using matrix doubling with a full relaxation matrix. T_1 leakage rates were set to 1 s^{-1}, cut-off distance to 5.5 Å, and τ_c was found to be optimal at 3.5 ns. Simulated spectra of the 200 ms NOESY experiments were calculated from these theoretical volumes using the program FELIX (Biosym). The back-calculated NOESY spectra were used to optimize the constraint file. The new constraint file was then used to create a new structure. These back-calculated refinement cycles were performed until the simulated NOESY cross-peak volumes matched the experimental data. In addition to visual matching of the cross-peak intensities, sometimes an *R*-factor, which sums the deviations between simulated and experimental cross-peaks, was calculated. However, this *R*-factor should be used with caution as a refinement parameter since intensities corresponding to short local sugar distances completely mask the intensities of weak cross-peaks that represent long-range global structure information. The program CURVES 5.3 was used to extract the helical parameters from the final structure.[15]

Acknowledgments

Financial support from the European Commission BIOMEDII program (Contract BMH4-CT97−2485) and Agence Nationale de Recherches sur le Sida is gratefully acknowledged. Thanks are ex-

tended to the Norwegian Research Council for a fellowship to B.A. We thank Dr. J. Arpalahti for carrying out additional HPLC and electrophoretic analysis.

[1] W. S. Marshall, M. H. Caruthers, *Science* **1993**, *259*, 1564−1570.
[2] C. A. Stein, Y. C. Cheng, *Science* **1993**, *261*, 1004−1012.
[3] P. S. Miller, *Prog. Nucleic Acids Res. Mol. Biol.* **1996**, *52*, 261−291.
[4] S. T. Crooke, *Med. Res. Rev.* **1996**, *16*, 319−344.
[5] S. Agrawal, *Trends Biotechnol.* **1996**, *14*, 376−386.
[6] C. Giovannangeli, C. Hélène, *Antisense Nucleic Acid Drug Dev.* **1997**, *7*, 413−421.
[7] R. W. Wagner, W. M. Flanagan, *Mol. Med. Today* **1997**, *3*, 31−38.
[8] Ciba Found. *Symp.* (Eds.: D. J. Chadwick, G. Cardew), John Wiley and Sons, Chichester, **1997**, vol. *209*.
[9] M. Boudvillain, R. Dalbies, M. Leng in *Metal Ions in Biological Systems* (Eds.: A. Sigel, H. Sigel), Marcel Dekker Inc., New York, **1996**, *33*, 87−102.
[10] K. M. Comess, C. E. Costello, S. J. Lippard, *Biochemistry* **1990**, *29*, 2102−2110.
[11] R. Dalbies, M. Boudvillain, M. Leng, *Nucleic Acids Res.* **1995**, *23*, 949−953.
[12] R. Dalbies, D. Payet, M. Leng, *Proc. Natl. Acad. Sci. USA* **1994**, *91*, 8147−8151.
[13] M. Boudvillain, M. Guerin, R. Dalbies, T. Saison-Behmoaras, M. Leng, *Biochemistry* **1997**, *36*, 2925−2931.
[14] C. Colombier, M. Boudvillain, M. Leng, *Antisense Nucleic Acid Drug Dev.* **1997**, *7*, 397−402.
[15] R. Lavery, H. Sklenar, CURVES 5.3 (http://www.ibpc.fr/UPR9080/CurForm bis.html)
[16] J. Lingbeck, M. G. Kubinec, J. Miller, B. R. Reid, G. P. Drobny, M. A. Kennedy, *Biochemistry* **1996**, *35*, 719−734.
[17] M. A. Lemaire, M. H. Fouchet, J. Kozelka, *J. Inorg. Biochem.* **1994**, *53*, 261−271.
[18] J. L. van der Veer, A. R. Peters, J. Reedijk, *J. Inorg. Biochem.* **1986**, *26*, 137−142.
[19] C. A. Lepre, K. G. Strothkamp, S. J. Lippard, *Biochemistry* **1987**, *26*, 5651−5657.
[20] F. J. Dijt, J. C. Chottard, J. P. Girault, J. Reedijk, *Eur. J. Biochem.* **1989**, *179*, 333−344.
[21] E. P. Nikonowicz, R. P. Meadows, D. G. Gorenstein, *Biochemistry* **1990**, *29*, 4193−4204.
[22] L. Joshua-Tor, D. Rabinovich, H. Hope, F. Frolow, E. Appella, J. L. Sussman, *Nature* **1988**, *334*, 82−84.
[23] V. P. Chuprina, E. Sletten, O. Y. Fedoroff, *J. Biomol. Struct. Dynam.* **1993**, *10*, 693−707.
[24] H. Huang, L. Zhu, B. R. Reid, G. P. Drobny, P. B. Hopkins, *Science* **1995**, *270*, 1842−1845.
[25] F. Paquet, C. Pérez, M. Leng, G. Lancelot, J. M. Malinge, *J. Biomol. Struct. Dynam.* **1996**, *14*, 67−77.
[26] F. Coste, J. M. Malinge, L. Serre, W. Shepard, M. Roth, M. Leng, C. Zelwer, *Nucleic Acids Res.* **1999**, *27*, 1837−1846.
[27] V. Sklenar, M. Piotto, R. Leppik, V. Saudek, *J. Magn. Reson. A* **1993**, *102*, 241−245.
[28] D. J. States, R. A. Haberkorn, D. J. Ruben, *J. Magn. Reson.* **1982**, *48*, 286−292.
[29] J. J. Led, H. Gesmar, *Chem. Rev.* **1991**, *91*, 1413−1426.
[30] *FELIX* (version 2.30) processing package, *Biosym/MSI*.
[31] *Bruker 1D WIN-NMR* (version 960901.2) and *2D WIN-NMR* (version 6.02).
[32] J. Kozelka, R. Savinelli, G. Berthier, J. P. Flament, R. Lavery, *J. Comp. Chem.* **1993**, *14*, 45−53.
[33] *BIOSYM* User Guide for *INSIGHT II* (version 2.3.5), *DISCOVER* (version 2.9.5) and *NMR Refine* (version 2.3).
[34] M. Jourdan, J. Garcia, E. Defrancq, M. Kotera, J. Lhomme, *Biochemistry* **1999**, *38*, 3985−3995.
[35] L. Verlet, *Phys. Rev.* **1967**, *159*, 98−103.
[36] H. J. C. Berendsen, J. P. M. Postma, W. F. van Gunsteren, A. DiNola, J. R. Haak, *J. Chem. Phys.* **1984**, *81*, 3684−3690.

Received December 4, 1999
[I00011]